High Performance 3U-Form Factor Pulsating Heat Pipe Heat Spreader

Sai Kiran Hota, Kuan-Lin Lee, Ramy Abdelmaksoud, Srujan Rokkam
Advanced Cooling Technologies, 1046 New Holland Ave Building 2
Lancaster, PA. USA. 17601
saikiran.hota@1-act.com; 717-205-0679

Abstract

Next generation electronics cards subjected to high heat fluxes must be effectively managed for reliable operation. To enable efficient thermal management, an additively manufactured Pulsating Heat Pipe (PHP) was investigated as a two-phase heat transfer electronics heat spreader for modular 3U form factor electronics. High performance was achieved with ammonia as the working fluid. Peak thermal performance determined for the PHP heat spreader was determined to be greater than 3.5 W/°C, which was about 3.3X higher than conduction plate. The PHP heat spreader was able to transport more than 450 W (~70 W/cm^2) without dry-out at lower condenser temperatures of -10°C. Additionally, it was estimated that the PHP heat spreader could yield up to 8% mass savings compared to conduction plate, which is critical for space applications.

Keywords

Heat spreader, thermal management, pulsating heat pipe, electronics cooling, two-phase cooling

Nomenclature

C	Thermal conductance (W/°C)
C_{pl}	Specific heat capacity in liquid form, (J/kg.K)
h_{fg}	Enthalpy of vaporization (J/kg)
M_{PHP}	Merit Number
Q	Heat (W)
R	Gas constant
T	Temperature (°C)
Z	Compressibility
σ	Surface tension (N/m)
μ	viscosity (Pa.s)
ϕ	Volume fill ratio
ρ	Density (kg/m^3)

1. Introduction

Recent trends in semiconductors have realized high computing electronics cards with small footprints. These high heat fluxes, must be effectively handled to maintain the electronics below 75-85°C for safe and reliable operation of the electronics card [1]. "Commercial" solutions employ conduction-based heat spreaders based on aluminum, copper, or even diamond, based on system limitations. However, the performance of these conduction cards is limited by material thermal conductivity, and thus are less feasible for application with next generation electronics dissipating very high heat fluxes, >> 10 W/cm^2. For a 1-inch x 1-inch footprint, the corresponding heat power is more than 65 W. In lieu of these thermal management challenges, two-phase heat spreaders, like Embedded copper-water Heat Pipes (EHP) [2], have been developed and fielded for electronics cooling. The EHPs have demonstrated between 2-8 times improvement in thermal performance for small form factor to larger 6U form factor electronics cards [2, 3, 4]. However, the freezing challenges with water as the heat pipe working fluid limits the application in situations where the heat spreader is exposed to temperatures ≤0°C like space environments. While freeze tolerant mixtures are explored, they are not reliable. Alternate working fluid like methanol cannot handle very large heat fluxes at low temperatures. A Pulsating Heat Pipe (PHP) heat spreader is a good alternative for such applications. PHP with appropriate working fluid enables efficient heat spreading of electronics cards in both near room temperature to low temperature environments. Here, the working fluid is typically a refrigerant like propylene, ammonia, or R134a [5, 6, 7, 8].

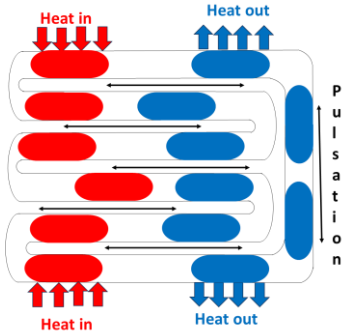

Figure 1. Schematic illustrating the operation of a PHP [9].

A PHP is a form of heat pipe where heat transfer occurs by means of liquid-vapor phase change and two-phase flow of the working fluid in capillary sized channels. Figure 1 shows the schematic of the operation of the PHP. The operation of the PHP is as follows [10, 11]: When heat is added (evaporator section), nucleation occurs through the liquid slug in the channels next to the heated wall resulting in an increase in the vapor pressure. Consequently, at the other end (condenser), the heat is delivered to the sink by the condensing vapor, which results in the reduction of vapor pressure. This dynamic interplay of the fluid pressures results in movement of the two-phase fluid in the capillary sized channels. PHPs have been investigated for use in varying extreme operating temperatures from cryogenics to ultra-high temperatures [12, 13] for applications in solar desalination [14], thermal management of electrical transformers [15], cooling of superconducting magnets [16], etc. Likewise, investigations have been ongoing on PHPs for electronics cooling like PHP-based heat spreaders. Similar to EHPs, research on PHPs based electronics cooling have 2 to 8 times improvement in small form factor electronics cards [17].

The PHP technology can be implemented for electronics cooling by integrating the fluid channels within the heat

spreader plate. A PHP heat spreader, additively manufactured with Al-6061 RAM2 for 3U form factor electronics is presented here, with ammonia as the working fluid. The manuscript is organized as follows: Section 2. describes fluid selection criteria; section 3. provides description of the PHP heat spreader along with test method; section 4. discusses experimental results; section 5. discusses ammonia-PHP (vessel) transportation requirements; and section 6. provides the conclusion.

2. PHP fluid selection

The PHP working fluid must satisfy the following primary constraints to be deemed as a suitable working fluid:

- Satisfy fluid channel diameter consideration by satisfying Bond number limitation, which when rearranged to determine the maximum diameter is given as [18]:

$$\boldsymbol{d_{cirt}(mm) = 2000 * \sqrt{\left(\frac{\sigma}{g(\rho_l - \rho_v)}\right)}} \quad \text{(eq.1)}$$

  Where, $\boldsymbol{\sigma}$ is the surface tension, $\boldsymbol{\rho_l}$ is the liquid density and $\boldsymbol{\rho_v}$ is the vapor density. The chosen PHP diameter was 1.52 mm.
- The working fluid must have high $\frac{dP}{dT}$ (at saturation) to enable high driving force within the fluid with low temperature drop.
- High PHP merit number to yield low thermal resistance [19].

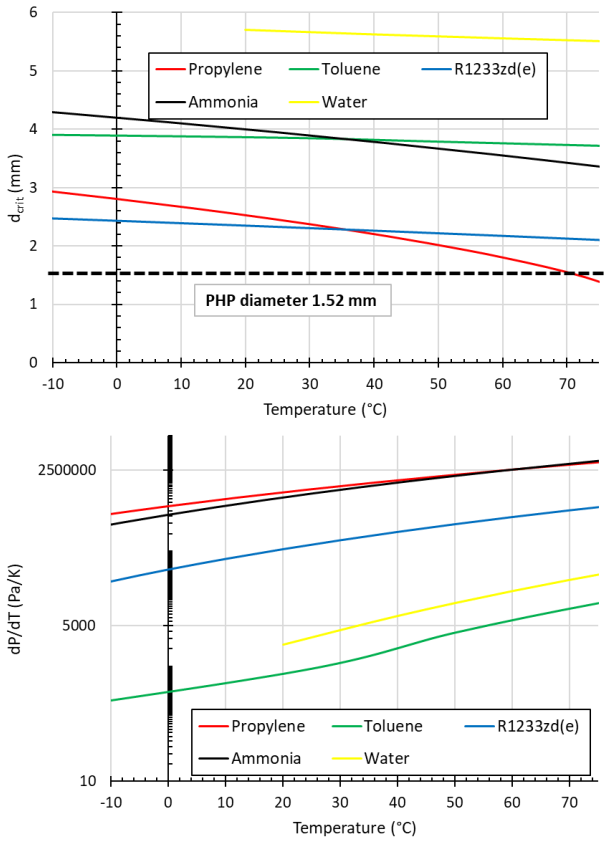

Figure 2. Critical diameter and dP/dT at saturation for PHP working fluids

Figure 2 shows the critical diameter and dP/dT of different classes of working fluids – refrigerants, toluene (organic compound) and water. Excluding propylene at very high temperatures, the working fluids easily meet the critical diameter requirement. However, the driving force potential by toluene and water are the lowest. Propylene, which was previously investigated as the working fluid for electronics cooling has the dP/dT on the order 1E6 Pa/K. Ammonia, likewise, has similar values as that of propylene. Based on these two aspects, both propylene and ammonia are suitable working fluids. However, fluid properties influencing the pulsation, as discussed below, indicate relative comparison of propylene and ammonia selection.

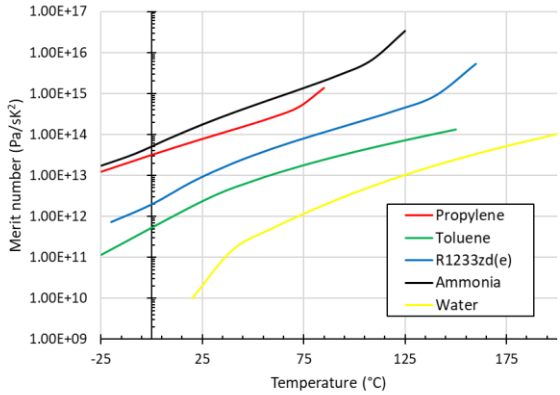

Figure 3. Merit number of PHP working fluids *[20]*

Figure 3 shows the merit number of PHP working fluids based on the performance (not heat transport limit). In addition to the driving force dP/dT, the merit number accounts for fluid density, specific heat capacity (C_{pl}), enthalpy of vaporization (h_{fg}), viscosity (μ_l), etc. all of which influence the pulsation (or circulation) of the working fluid within the channels as fluidic forces. The merit number is given as [19]:

$$M_{PHP} = \frac{\rho_l C_{pl}\left(\frac{dP}{dT}\right) ZRT}{\mu_l h_{fg}} \quad \text{(eq.2)}$$

Based on the above calculation, it was determined that the merit number of ammonia was higher than propylene, while, the merit number of all other fluids were several orders of magnitude lower. In addition to the above three selection criteria, typically, the heat transfer limits of the working fluids were estimated to further support fluid selection. Heat transfer limits are often calculated to estimate the maximum heat load the two-phase technology can deliver. This often varies with temperature and the fluid being used. When the fluid is near the freezing point, often viscous and sonic limit dictate the maximum heat transfer rate, however, in the current context they do not feature. For PHP, maximum heat transfer rate is associated with vapor-inertial limit and corrected with swept-length limit at higher operating temperature range. Vapor-inertial limit occurs when the vapor plug starts to penetrate into the slug causing the breakage of slug-plug pair. Swept-length limit is attributed to the relationship between the heated length and the liquid slug-length to cover the heater section to maintain the fluid nucleation rate for boiling/ vaporization. In the PHP heat transfer limits proposed by Drolen and Smoot [21], it was noted that identifying appropriate number of turns

in a PHP heat spreader within a highly conductive plate like aluminum is difficult and could result in heat transfer limits discrepancy. However, from preliminary calculations, it was computed that the heat transfer limits for propylene varied from ~250W at 10°C to below 100W at 40°C, to below 10W at 60°C. Some of the operational data points and dry-out values were correlated to the heat transfer limits experimentally with reasonable accuracy [20]. Using these models, the estimated heat transfer limits of ammonia were determined to be higher than propylene, reaching a value significantly greater than 500W at a temperature above 40°C. Investigating these heat transfer limits the following inferences can be drawn: the typical maximum heat transfer limit of PHP given by the vapor-inertial limit is higher with ammonia compared to propylene; and the influence of the swept length limit is witnessed in temperature ~ 45°C with propylene, while, for ammonia, it does not appear until above 70°C. With regards to heat transfer potential, this indicates ammonia is a highly suitable PHP working fluid for electronics cooling in comparison to alternative options like propylene.

3. Description of heat spreader and testing methodology

A 3U form factor PHP heat spreader was fabricated for 3U form factor electronics cards, of dimensions 160 mm x 100 mm x 3.38 mm. The capillary PHP fluid channels were formed with a diameter of 1.52 mm. Figure 4 shows the geometric information on the additively manufactured PHP heat spreader. The material used for fabrication was Al-6061 RAM2. To facilitate fabrication and charging of the working fluid, powder removal ports were integrated within the plate. After fabrication, excess powder was removed and welded shut. The working fluid was charged through the fill tube port. The performance of the PHP heat spreader was compared against solid aluminum-conduction plate of similar dimensions. The conduction plate was made fabricated by CNC machining with Al-6061. The theoretical thermal conductivity of the heat spreader was 167 W.mK, which returns a thermal conductivity of 1.14 W/°C. Experimental thermal conductance of the conduction plate was 1.1±0.1 W/°C.

Quasi steady state test method was adopted for performance testing of the PHP heat spreader using a central heat in with two edge heat-out method. A 25.4 mm x 25.4 mm (1-inch x 1-inch) aluminum block with cartridge heater rod inserts was used to simulate the electronics heat source. Three thermocouples were attached to the heat spreader at the heater block interface using plunger thermocouples with springs providing constant pressure. Two cold plates attached to the two edges of the heat spreader through wedge-lok card retainers [22] were used as heat sinks for heat PHP heat rejection. Liquid Nitrogen (LN) was circulated through the cold plate for heat removal. A solenoid valve was used to continuously obtain feedback from the PHP condenser thermocouple to maintain constant temperature (referred to as operating temperature here). The overall test setup is shown in Figure 5. The test fixture was insulated using fiberglass insulation on the heat spreader and the heater block and a 1-inch thick garolite foam insulation was put around the test block.

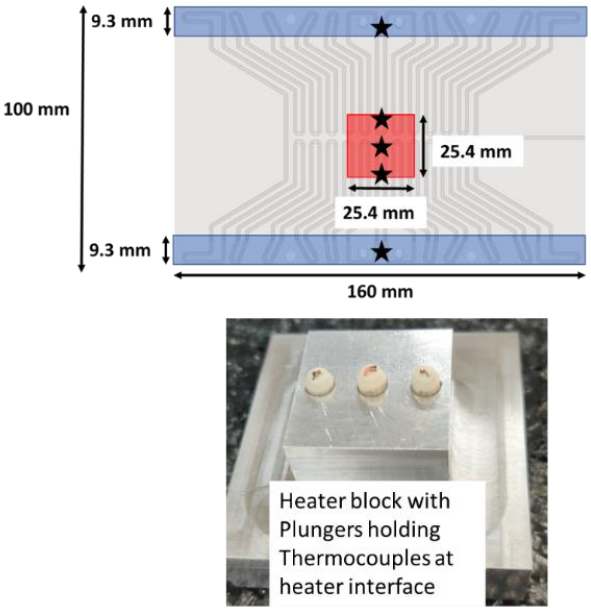

Figure 4. Channel layout geometry, and testing method for characterizing performance of PHP heat spreader. The bottom of the schematic shows heater block with plungers holding thermocouples at the heater-PHP heat spreader interface to record evaporator temperature.

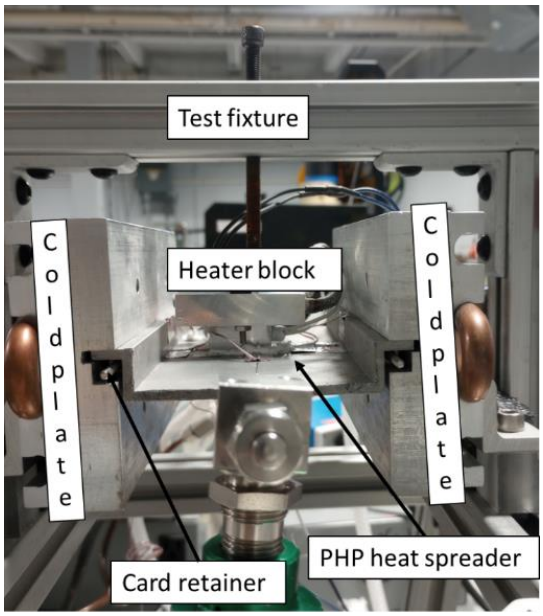

Figure 5. PHP heat spreader test fixture

The thermal performance was determined as the thermal conductance (C), calculated as:

$$C = \frac{Q}{\Delta T} \quad \text{(eq.3)}$$

Where, Q is the heat input and ΔT is steady state temperature difference between the average evaporator temperature and the condenser temperature. The experiments

were performed three times at each data point for repeatability. At highest heater power of ~450W, the maximum variation in the heat input was ±3.5W, and estimated power loss through the insulation using equivalent heat transfer coefficient of ~5 W/m^{2}K was 6.4W. Total uncertainty in heat input was 2.2% at highest heat input. The uncertainty in thermocouples was ±0.5°C. The variation in uncertainty of thermal conductance based on the formulation presented by [23] was calculated to be 2.5%.

The thermal performance testing of the PHP heat spreader was undertaken with fluid fill ratios of 50% and 75% (reference at 22°C) with condensers maintained in the temperature range of -10°C to +30°C in horizontal and vertical configuration. The PHP was charged with ammonia at -23°C to reduce effects of high-pressure fluid in the charging tubes at room temperature.

4. Thermal performance of PHP plate heat spreader

4.1 Thermal performance of PHP at 50% fill ratio

The PHP heat spreader was tested at 50% fill ratio (@22°C) in quasi-steady state method. The temperature profiles Figure 6 and Figure 7 shown below corresponds to condenser temperatures of -10°C and +20°C, respectively.

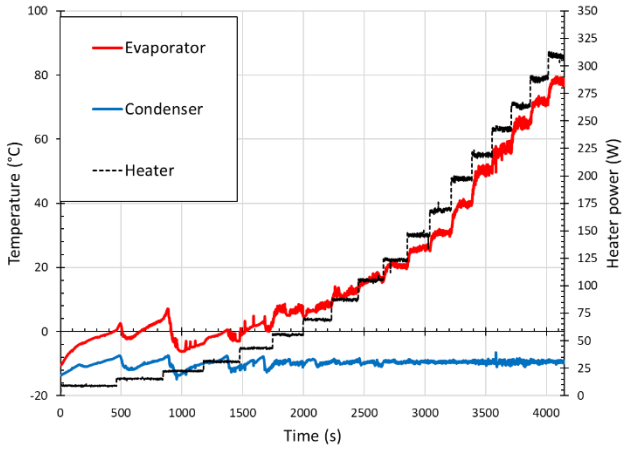

Figure 6. PHP heat spreader temperature profile with condenser at -10°C

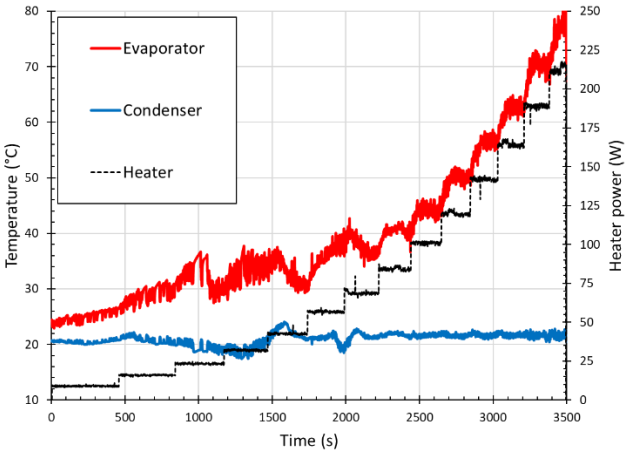

Figure 7. PHP heat spreader temperature profile with condenser at 20°C

Figure 6 and Figure 7 show the PHP wall temperature at condenser temperature of -10°C and +20°C, respectively in horizontal configuration. At lower heater powers, some variation in condenser temperature was observed due to delay in the PID learning curve of the solenoid valve and the high thermal mass discrepancy of cold plates. At low condenser temperature, a start-up power of ~30W was required for the two-phase operation of the PHP to initiate. As the heater power increased, especially above 50W, the pulsation on the wall evaporator temperature became more consistent with pronounced two-phase operation. The PHP could transport ~310W (48 W/cm^2) without dry-out, with the evaporator reaching a temperature of about 80°C. As the condenser temperature increased to +20°C, easier start-up in the PHP was obtained. The PHP could deliver 210W (32.5 W/cm^2) without dry-out. The corresponding evaporator temperature was 78°C. The testing was stopped above this point for equipment safety and to avoid very high pressures within the PHP.

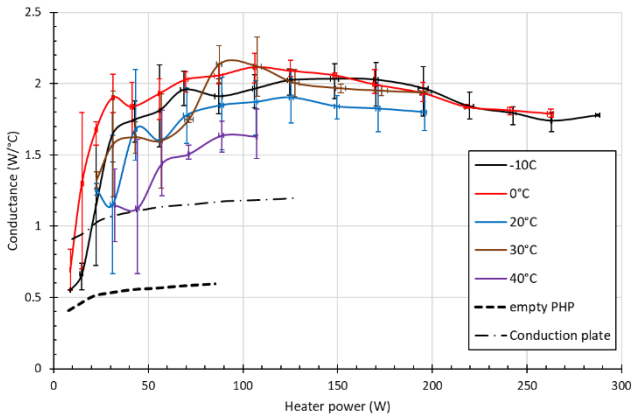

Figure 8. Thermal conductance of the PHP heat spreader at 50% volume fill ratio in horizontal configuration

Figure 8 shows the thermal conductance of the ammonia PHP heat spreader at 50% volume fill ratio. Additionally, testing was performed at condenser temperature of +40°C (for this data set only). The thermal conductance of the PHP increased gradually from below 1 W/°C (before or just after start-up) to above 2 W/°C (~2X conduction plate and ~3.9X empty PHP). At condenser temperatures of -10°C and 0°C, the thermal conductance was consistently above 2 W/°C until heater power of 200W. Above 200W heater power, a small decline in the thermal conductance was observed. This can be attributed to change in the fluid flow pattern (oscillation to circulation) or departure from slug to flow to other flow patterns. It can also be attributed to the fact that the "vapor quality" increases at higher powers, and the flow patterns vary with increasing vapor quality. High vapor quality leads to annular flow, which, in the case of PHP represents dry-out condition. In the case of PHPs, slug flow is vital for consistent operation of the PHP [24]. As the condenser temperature increased to +30°C or even +40°C, it was deduced that the peak thermal conductance decreased, and the performance improvement compared to conduction card was typically lower than 1.5X. This can be attributed to both changes in the vapor

quality and dynamic change in the instantaneous fluid ratio because of changes in the liquid/vapor density of ammonia.

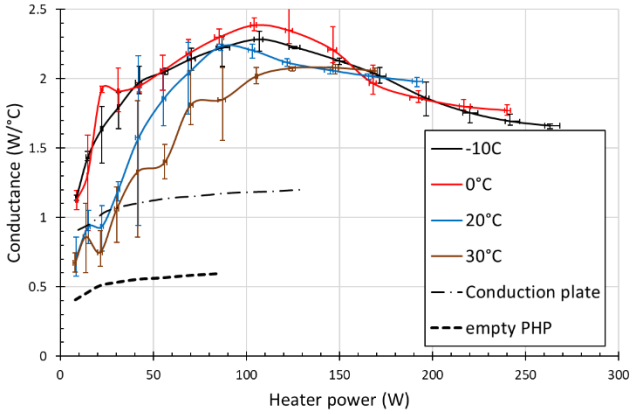

Figure 9. Thermal conductance of the PHP heat spreader at 50% volume fill ratio in vertical configuration

Likewise, performance testing of the PHP heat spreader was undertaken in vertical configuration. Figure 9 shows the thermal conductance of the PHP heat spreader in vertical configuration. At low heater powers, it was observed that the thermal conductance was marginally greater than that of the horizontal configuration. The peak thermal conductance greater than 2.2 W/°C was obtained at low condenser temperatures of -10°C and 0°C. However, as the heater power increased to above 175W, the thermal conductance reduced to a value of ~1.6-1.8 W/°C. In general, vertical orientation assisted with the PHP start-up by supporting fluid motion. However, at higher power, lower thermal conductance was observed in comparison to horizontal configuration due to the aforementioned reasons.

4.2 Thermal performance of PHP at 75% fill ratio

The PHP was tested at higher fluid fill ratio of 75% (@22°C) at similar condenser temperatures in the range -10°C to +30°C in both horizontal and vertical configuration.

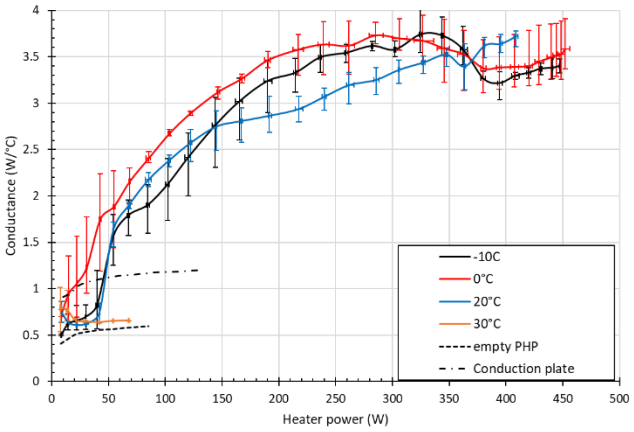

Figure 10. Thermal conductance of the PHP heat spreader at 75% volume fill ratio in horizontal configuration

Figure 10 shows the thermal conductance of the PHP heat spreader with ammonia charged at 75% fill ratio in horizontal configuration. The thermal conductance increased from below 1W/°C to more than 3.5 W/°C at condenser temperatures of -10°C to +20°C. The thermal performance improvement of the heat spreader was about 3.3X conduction plate and 6.5X empty PHP. The PHP was able to deliver more than 400W (62 W/cm^2) and up to 450W (~70 W/cm^2) without dry-out. The maximum evaporator temperature was determined to be ~60°C. Further testing was limited by the heater power limitations of the cartridge heater. However, at a higher condenser temperature of +30°C, the PHP failed to operate. As mentioned in the previous section, this can be attributed to the instantaneous change in the fluid fill ratio with the corresponding PHP temperature. The highest performance was obtained for the PHP heat spreader with this condition. However, in one setting when the fluid fill ratio increased to 80%, the PHP did not operate. The influence of the fluid fill ratio is discussed in the subsequent sub-section.

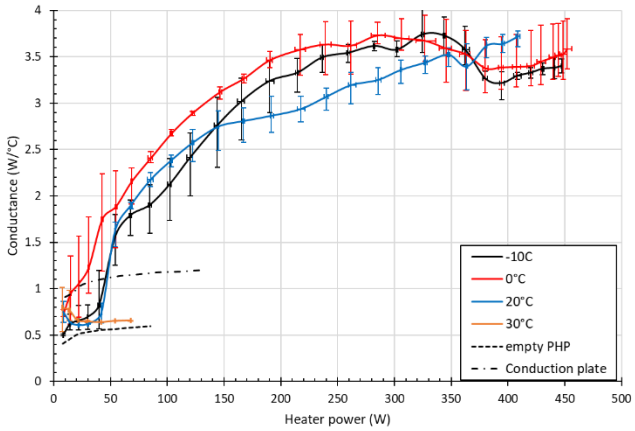

Figure 11. Thermal conductance of the PHP heat spreader at 75% volume fill ratio in vertical configuration

Figure 11 shows the thermal conductance of the PHP heat spreader in the vertical configuration. Interestingly, the peak thermal conductance was marginally lower in comparison to the horizontal configuration, demonstrating some of gravity in the PHP heat spreader thermal performance. This was furthermore elucidated by the non-operational PHP at 20°C condenser temperature, which was otherwise operational in the horizontal case. At higher fill ratio, the longer liquid slug experiences greater gravitational force in comparison to lower fill ratios, although the preferred-direction of fluid movement could not be ascertained here. The peak thermal conductance obtained here was ~3.3-3.4 W/°C, which was almost 0.3W/°C lower than the horizontal case. The vertical orientation hampered the thermal conductance to certain extent in this case. Although the PHP heat spreader was able to transport up to 450W heat, the maximum evaporator temperature obtained here was up to 80°C. The improvement in thermal performance over conduction plate and the empty PHP was 3X and 6X, respectively.

4.3 Evaluating influence of fluid fill ratio on PHP thermal performance

From above analysis, it was deduced that the fluid fill ratio of 50% experienced faster start-up, the peak thermal

conductance obtained was between 2.1-2.3 W/°C for chosen condenser temperature range from -10°C to +30°C in both horizontal and vertical configuration. Within the heat power range of 75-200W, the thermal conductance trend was almost similar and some variation in the performance, up to ±0.3W/°C or higher was observed at lower or higher heater powers for a given condenser temperature (from Figure 8 and Figure 9). As noted, at lower heater powers, at nominal fill ratio of 50%, gravity assists with fluid circulation and supports PHP start-up at lower condenser temperatures. Despite variation in thermal performance, the operation of the PHP heat spreader was less sensitive to gravity at 50% fill ratio.

However, at higher fill ratio of 75%, influence of gravity was noted at higher heater powers and at condenser temperature of +20°C and above. Higher fill ratio corresponds to longer liquid slugs, which experience higher gravitational force in comparison to other fluidic forces like viscous force or vapor expansion force, etc. At higher PHP temperatures resulted by higher heater powers, the weakening surface tension coupled with these forces further influences the fluid movement in vertical orientation in comparison to the horizontal configuration. While, high fluid velocity is desired, very high fluidic velocity is detrimental as it influences the pressure drop.

While, both 50% and 75% fill ratio showed significant improvement in PHP heat spreader performance, testing was performed at lower fluid fill ratio of 25% - smaller liquid slugs.

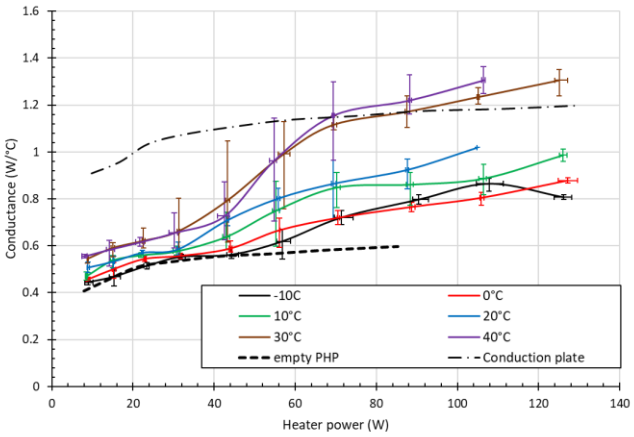

Figure 12. Thermal conductance of the PHP heat spreader at 25% volume fill ratio in horizontal configuration

Figure 12 shows the thermal conductance of the PHP heat spreader at low fill ratio of 25% (undercharged condition). As observed, although, two-phase operation was obtained, the uncertainty in the presence of the liquid slug and the instantaneous fluid velocity (and thereby the vapor quality) variation resulted in poor performance. Overall, the thermal conductance of the PHP heat spreader in the undercharged condition was poorer than or comparable to the conduction plate, based on the heater power and the operating condition.

While, undercharged fluid lends to poor PHP thermal performance, it was determined that higher fill ratio of 75% is suitable for PHP at low condenser temperatures. At higher condenser temperatures, for any given power, if the instantaneous fill ratio is higher than the maximum theoretical value, then the PHP does not operate. For example, the instantaneous fill ratio was 77% for PHP temperature of 30°C, but the theoretical maximum at the same temperature was 76.4%. The theoretical maximum ($\boldsymbol{\phi_{max}}$) was calculated as [25]: $\boldsymbol{\phi_{max}} = \frac{1}{1+\left(\frac{kRT\rho_l}{K}\right)^{0.5}}$, Where, $\boldsymbol{k}$ is the adiabatic coefficient and $\boldsymbol{K}$ is the bulk modulus.

4.4 Comparison of thermal performance of ammonia PHP against literature data on propylene PHP and EHP

The thermal conductance of the PHP heat spreader with ammonia was compared against propylene PHP and EHP for similar geometry [6, 11]. The propylene PHP performance was tested at -10°C to +30°C and the EHP was tested at +20°C. The EHP had 4 U-shaped Cu-H_2O heat pipes.

Table 1. Thermal performance comparison of ammonia PHP against propylene PHP and EHP discussed in literature

Heat Spreader	Improvement in C over conduction plate	Maximum Power (dry-out/ tested) [W]	Relative mass change
Conduction plate	-	150	-
Propylene PHP (50%	~1.3-1.4X	210	-8.5%
Propylene PHP (75%)	1.5-2X	260	-8%
EHP	2X	260	+2.2%
Ammonia PHP (50%)	1.7-2X	260	-8.3%
Ammonia PHP (75%)	3-3.3X	450	-7.75%

Table 1 shows the thermal performance comparison of ammonia PHP (discussed here) against propylene PHP in the temperature range -10°C to +20°C and EHP at +20°C. In general propylene PHP at higher fill ratio and EHP showed up to 2X improvement against conduction plate [6, 11]. The ammonia PHP at nominal 50% fill ratio presented similar performance improvement, but higher fill ratio of 75% showed pronounced thermal conductance improvement by 3.3X over conduction plate with capability of delivering more than 450W heat (70 W/cm^2 heat flux) without dry-out. Another advantageous feature of PHP is mass savings. The PHP, with the current channel design saves up to 8% in mass in comparison to conduction card (~184.2 grams). This is an important criterion for space electronics cards. In contrast, EHP showed a slight increase in mass by 2.25%.

5. Transporting ammonia-PHP (heat spreader)

Ammonia PHP was determined to be high performance thermal heat spreader for electronics cooling. However, ammonia is classified as a toxic gas by the Department of Transportation (DOT) under hazard class 2.3 (UN 1005). The transportation of the heat spreader from the manufacturing facility to the recipient must meet stringent guidelines. The heat spreader envelope treated as a pressure vessel must meet following pressure safety criteria [26, 27, 28].

- The fluid container must be designed to minimum packaging pressure no less than 1.5 times vapor pressure at 46°C, which is 2750 kPa.
- ASME recommends safety pressure check up to 4 times the maximum fluid pressure, which is expected to be ~10350 kPa.
- DOT-SP 11818 recommends testing up to 1400 Psi (9650 kPa).

The saturation temperature for ammonia at 2750 kPa is 62°C. The PHP heat spreader was repeatedly tested to temperature above 80°C in several instances. In addition, at the start, the PHP heat spreader was tested with nitrogen gas up to a pressure of 10350 kPa.

Every manufacturer maintains a record of components with ammonia fluid and the recipient can discuss requisite information as desired. Usually, ammonia vessels can only be shipped in cargo carriers following DOT permit authorization DOT-SP 11818. The safety measures in the permit indicate protocols for packaging and testing the heat spreader welds (ASTM E-1742, NAS1514, or equivalent).

Figure 13. Warning signs and labels required to indicate the shipment contains ammonia.

The packaging box must properly contain the heat spreader within it and have precautionary labels and signs, like the photograph shown in Figure 13. The warning labels shown here indicate, inhalation hazard & toxicity category 3, cargo-aircraft only, environment hazard, and corrosion and skin irritation. Shipment destinations and modes mandate the use of some of these warning labels. Usually ground or ocean shipment is preferred, but in air transportation, the ammonia filled heat spreader (container) can only be transported in cargo. For domestic (within U.S.A) transportation, non-flammable gas green class 2.2 sticker is used. International shipment must contain corrosion and inhalation hazard stickers. Poison/ toxicity stickers are particularly required for ocean transportation.

6. Conclusions

Thermal performance characterization of ammonia charged PHP heat spreader at fill ratios of 50% and 75% is presented at various condenser temperatures in the range -10°C to +30°C. The dimensions of the heat spreader were 160 mm x 100 mm x 3.38 mm with fluid channel diameter of 1.52 mm. Tests were performed using a central 25.4 mm x 25.4 mm heater block with two edge condensers through a cold plate interfaced with wedge-lok card retainer. Following inferences were drawn:

At nominal fill ratio of 50%, peak thermal conductance up to 2.1±0.1 W/°C was obtained in the heater power range 75-200W. This was about 2X compared to conduction plate. At higher power loads, a slight reduction in thermal conductance to 1.8 W/°C was obtained. The thermal conductance of the PHP heat spreader in both horizontal and vertical orientation showed similar trend with small differences. The PHP heat spreader operated effectively in all condenser set points from -10°C to +30°C.

At higher fluid fill ratio of 75%, the thermal conductance of the PHP heat spreader further pronounced to values > 3W/°C. Peak thermal conductance >3.5W/°C was obtained in horizontal orientation. The increase in thermal conductance compared to the conduction plate was 3.3X. The PHP was able to deliver more than 450 W (70 W/cm^2) without dry-out at operating (condenser) temperatures of -10°C and 0°C. In vertical orientation, some slight influence of gravity was observed, potentially due to larger liquid slug length, coupled with high instantaneous fill ratio for a given heat load. However, the vertical orientation also demonstrated high thermal conductance, up to 3X more than conduction plate. In the horizontal orientation, the PHP heat spreader did not operate at +30°C set point, while in vertical orientation, the PHP heat spreader did not operate at +20°C and +30°C condenser set points.

While, significant improvement in thermal conductance was obtained with PHP heat spreader, it was deduced that ammonia as working fluid was suitable for condenser temperatures below +30°C. While, the PHP showed improvement in performance at +40°C at 50% fill ratio, the improvement in thermal conductance compared to the conduction plate was less than 1.5X.

When compared to past published literature on similar geometry, ammonia as the working fluid showed more suitability compared to propylene. Furthermore, it was determined that PHP could yield mass savings in the electronics card, which is an important criterion for consideration for space applications.

Acknowledgments

This work was performed with the support of NASA's Small Business Innovation Research (SBIR) Phase II contract #80NSSC22CA205. The authors are grateful to Dr. Sergey Y.

Semenov for his support. The authors express their gratitude to the engineering technician, Mr. Eugene Sweigart and Mr. Phil Texter for their support with fabrication and experiments. The authors also thank ACT's Operations team for their support with welding tasks. Authors thank Mr. Brad Hartzler, shipping and receiving manager at ACT.

References

[1] S. Murshed and C. de Castro, "A critical review of traditional and emerging techniques and fluids for electronics cooling," *Renewable and Sustainable Energy Reviews,* vol. 78, pp. 821-833, 2017.

[2] K.-L. Lee, S. K. Hota, A. Lutz and S. Rokkam, "Advanced two-phase cooling system for modular power electronics," in *51st International Conference on Environmental Systems*, St. Paul, MN, 2022.

[3] S. K. Hota, K.-L. Lee, G. Hoeschele, R. W. Bonner and S. Rokkam, "Performance investigation on different form factor embedded heat pipe and pulsating heat pipe heat spreaders," in *Proceedings of 17th International Heat Transfer Conference*, Cape Town, South Africa, 2023.

[4] S. K. Hota, K.-L. Lee, G. Hoeschele, R. Bonner and S. Rokkam, "Experimental comparison on thermal performance of pulsating heat pipe and embedded heat pipe heat spreaders," in *2023 39th Semiconductor Thermal Measurement, Modeling & Management Symposium (SEMI-THERM)*, San Jose, CA, 2023.

[5] Im, Y. Hoon, J. Y. Lee, Ahn, T. In, Youn and Y. Jik, "Operational characteristics of oscillating heat pipe charged with R-134a for heat recovery at low temperature," *International Journal of Heat and Mass Transfer,* vol. 196, p. 123231, 2022.

[6] S. K. Hota, Lee, Kuan-Lin, G. Hoeschele and S. Rokkam, "Investigation on Pulsating Heat Pipe (PHP) Heat Spreader Plate for Electronics Cooling," in *2024 40th Semiconductor Thermal Measurement, Modeling & Management Symposium (SEMI-THERM)*, San Jose, CA, 2024.

[7] N. Van Velson, R. Kumar, C. Tarau and G. F. Moroni, "Thermal Management of Large Area Heat Loads Using Multi-Pass Cryogenic Loop Heat Pipe," in *AIAA SCITECH 2024 Forum*, 2024.

[8] Hu, Lingfeng, Y. Chen, C. Wu and H. Zhang, "Optimization design and performance analysis of ammonia heat pipe air heater under low ambient temperature conditions," *Applied Thermal Engineering,* vol. 225, p. 120202, 2023.

[9] S. K. Hota, K.-L. Lee, T. McFarland, G. Hoeshcele, J. Weyant and S. Rokkam, "High performance heat spreader for thermal management of high heat flux optical and electronics systems," in *Next-Generation Optical Communication: Components, Sub-Systems, and Systems XIII*, San Francisco, CA, 2024.

[10] V. S. Nikolayev and M. Marengo, "Pulsating heat pipes: basics of functioning and modeling," in *ENCYCLOPEDIA OF TWO-PHASE HEAT TRANSFER AND FLOW IV: Modeling Methodologies, Boiling of CO_2, and Micro-Two-Phase Cooling Volume 1: Modeling of Two-Phase Flows and Heat Transfer*, World Scientific, 2018, pp. 63-139.

[11] S. K. Hota, K.-L. Lee, G. Hoeschele, T. Mcfarland, S. Rokkam and R. Bonner, "Experimental comparison of two-phase heat spreaders for space modular electronics," in *2023 International Conference on Environmental Systems*, 2023.

[12] L. Kossel, J. Pfotenhauer and F. Miller, "Thermal performance and stability experiments of a 1.75-meter-long helium pulsating heat pipe," in *IOP Conference Series: Materials Science and Engineering*, 2024.

[13] D. Takouda and T. Inoue, "Heat transport characteristics of a sodium oscillating heat pipe: thermal performance," *International Journal of Heat and Mass Transfer,* vol. 196, p. 123281, 2022.

[14] H. Abad, M. Ghiasi, S. Mamouri and M. Shafii, "A novel integrated solar desalination system with a pulsating heat pipe," *Desalination,* vol. 311, pp. 206-210, 2013.

[15] R. Abdelmaksoud, J. Diebold, S. K. Hota, K.-L. Lee, S. Sinha and D. Maksimovic, "Development of ceramic pulsating heat pipes for medium-voltage power electronics," in *International Electronic Packaging Technical Conference and Exhibition*, San Diego, CA, 2023.

[16] K. Natsume, T. Mito, N. Yanagi, H. Tamura, T. Tamada, K. Shikimachi, N. Hirano and S. Nagaya, "Heat transfer performance of cryogenic oscillating heat pipes for effective cooling of superconducting magnets," *Cryogenics,* vol. 51, no. 6, pp. 309-3014, 2011.

[17] S. K. Hota, K.-L. Lee, B. Leitherer, G. Elias, G. Hoeschele and S. Rokkam, "Pulsating heat pipe and embedded heat pipe heat spreaders for modular electronics cooling," *Case Studies in Thermal Engineering,* vol. 49, p. 103256, 2023.

[18] M. Fazli, S. Mehrjardi, A. Mahmoudi, A. Khademi and M. Amini, "Advancements in pulsating heat pipes: Exploring channel geometry and characteristics for enhanced thermal performance," *International Journal of Thermofluids*, vol. 22, p. 100644, 2024.

[19] J. Kim, Kim and S. Jin, "Experimental investigation on working fluid selection in a micro pulsating heat pipe," *Energy Conversion and Management,* vol. 205, p. 112462, 2020.

[20] S. K. Hota, K.-L. Lee, G. Hoeschele, T. McFarland and S. Rokkam, "Development of Modular 3U Form Factor Pulsating Heat Pipe Based Plate Heat Spreader for Electronics Cooling," in *53rd International Conference on Environmental Systems*, Louisville, USA, 2024.

[21] B. Drolen and C. Smoot, "Performance limits of Oscillating Heat Pipes: Theory and Validation,"

Journal of Thermophysics and Heat Transfer, vol. 31, no. 4, 2017.

[22] https://www.1-act.com/thermal-solutions/embedded-computing/ice-lok/?srsltid=AfmBOopZ_isd2wp3-DmvjQoLOuBjarpGaDUOzLXaNfSZdCOyEYOrZiFv.

[23] D. Liu, J. Liu, K. Yang, F. Shang, C. Zheng and X. Cao, "Evaluation of the Heat Transfer Performance of a Device Utilizing an Asymmetric Pulsating Heat Pipe Structure Based on Global and Local Analysis," *Energies*, vol. 17, no. 22, 2024.

[24] Z. Li, "Study of a Hybrid of Pulsating Heat Pipe and Distributed Jet Array," *Journal of Thermophysics and Heat Transfer*, vol. 34, no. 2, 2020.

[25] D. Yin, H. Rajab and H. Ma, "Theoretical analysis of maximum filling ratio in an oscillating heat pipe," *International Journal of Heat and Mass Transfer*, vol. 74, pp. 353-357, 2014.

[26] https://www.ecfr.gov/current/title-49/subtitle-B/chapter-I/subchapter-C/part-173/subpart-G/section-173.315.

[27] https://info.thinkcei.com/think-tank/asme-standards#:~:text=Previous%20years%20of%20ASME%20Standards,can%20create%20a%20custom%20material..

[28] https://www.phmsa.dot.gov/hazmat/documents/offer/SP11818.pdf/offerserver/SP11818.